Tamaki, K., Suyehiro, K., Allan, J., McWilliams, M., et al., 1992
Proceedings of the Ocean Drilling Program, Scientific Results, Vol. 127/128, Pt. 2

72. SEISMIC STRATIGRAPHY OF THE KITA-YAMATO TROUGH[1]

P. R. Holler[2] and K. Suyehiro[1]

ABSTRACT

The analysis of high resolution seismic reflection data from the Kita-Yamato Trough enabled us to differentiate five seismic intervals above acoustic basement. In order to correlate the borehole information from Site 799 with the seismic field record, synthetic seismograms were calculated from physical property data. Using borehole data it is possible to correlate seismic and lithologic units.

The reflection patterns of seismograms from other parts of the Japan Sea are very similar to those from the Kita-Yamato Trough. This indicates that the local results from the Kita-Yamato Trough can be used to explain the geology on a more regional scale.

INTRODUCTION

The Kita-Yamato Trough represents a major structural and topographic depression which divides the Yamato Rise along a northeast-southwest trend (Fig. 1). Seismic reflection records which cross the trough show it to be a graben with the thickest sediment column confined to the narrow central portion of the structure (Tamaki, 1988). All records show that acoustic basement is offset by the apparent faults demarking the sides of the trough. Uplifted acoustic basement is most apparent beneath the Yamato and Kita-Yamato banks flanking the trough. Seismic records also demonstrate that acoustic basement deepens slightly northeastward toward the center of the trough and then becomes shallower again.

Ocean Drilling Program (ODP) Leg 128 drilled a 1084 m deep hole at Site 799 (Fig. 1) in the central part of the Kita-Yamato Trough (Shipboard Scientific Party, 1990c). The sedimentary column at Site 799 was divided into five lithostratigraphic units based on shipboard analysis of lithologic composition and variability, sedimentary structures, and diagenetic alteration as shown in Figure 2.

After drilling at Site 799, a seismic survey was conducted in the same manner as the site approach (Fig. 3). The purpose of this survey was to tie the record obtained by drilling with seismic information on the trough and the ridges in order to assemble a three-dimensional view of the Kita-Yamato Trough.

The aim of this paper is to correlate borehole lithology with reflection seismic records from the Kita-Yamato Trough. In order to perform this correlation a geologic model is constructed by means of physical properties data from laboratory measurements and downhole measurements.

METHODS

Seismic Reflection Data

The seismic reflection data were collected aboard *JOIDES Resolution* during ODP Leg 128 in the Kita-Yamato Trough (Fig. 3).

Two 80 in.3 (1300 cm^3) Seismic System Inc. (SSI) water guns were used as a seismic source. They were operated at a pressure of 1700–2000 psi (120–140 bar) and towed at a depth of about 10 m below sea level (mbsl). The shot interval was 12 s, the ship's speed during the survey was 6 kt (11 km/hr or 3.1 m/s). So the distance between two shotpoints is 37 m.

The streamer we used is a 100 m long Teledyne streamer with 60 active sections. The streamer was towed 500 m behind the vessel at a depth of 10 mbsl. A 25 m long stretch section was put between the lead-in cable and the streamer cable.

The analog data were first bandpass-filtered. Then the data were digitized and recorded in the SEGY format on tape for further processing such as deconvolution, etc.

Physical Property Data

The physical property program during Leg 128 included the determination of index properties like wet-bulk density, water content, porosity, dry-bulk density, and grain density; the determination of *P*-wave velocity, thermal conductivity, and undrained shear strength. The techniques are described in detail by, e.g., Boyce (1976), Shipboard Scientific Party (1990a), and Nobes et al. (this volume).

Mayer et al. (1986) pointed out that wet-bulk density and sonic velocity are the most important physical properties for seismic modeling. The product of these two properties is the acoustic impedance. Contrasts in the acoustic impedance are responsible for seismic reflectors. Therefore the methods for the determination of wet-bulk density and *P*-wave velocity will be reviewed.

Wet-bulk density is defined as the ratio between the weight of the wet sample and the volume of the wet sample. During Leg 128 the wet volume of the sample was determined using a helium displacement pycnometer, the weight was determined using a Scientech electronic balance (Shipboard Scientific Party, 1990a). As pointed out by Nobes et al. (this volume), a systematic error was determined for the wet volume determination. However, in this paper we use the uncorrected wet-bulk densities, because the systematic error does not affect the relative contrasts in the downsection density profile. These relative contrasts in wet-bulk density are much more important for seismic modeling than the absolute wet-bulk densities, because they can influence the acoustic impedance contrast and create reflectors on seismic records.

P-wave velocity was determined by the continuous *P*-wave logger, the Hamilton frame velocimeter, and downhole measurements (Shipboard Scientific Party, 1990a; Borehole Research Group, 1987). The sediments recovered from Site 799 were strongly degassing. So data obtained by the *P*-wave logger are restricted to the upper 50 m of section, and velocimeter determinations were restricted to the lower part of section (below 500 mbsf). *P*-wave velocities from downhole measurements are available in the depth range between 110 and 1049 mbsf. The values for the *P*-wave velocity of the depth range between 50 and 110 mbsf were estimated. *P*-wave velocities from downhole measurements are not influenced by changes in temperature, the decrease of hydrostatic pressure, porosity rebound, or decrease in rigidity due to the removal of the cores from *in-situ*

[1] Tamaki, K., Suyehiro, K., Allan, J., McWilliams, M., et al., 1992. *Proc. ODP, Sci. Results,* 127/128, Pt. 2: College Station, TX (Ocean Drilling Program).
[2] Geologisch-Paläontologisches Institut der Universität Kiel, Olshausenstrasse 40-60, 2300 Kiel, Federal Republic of Germany.
[3] Ocean Research Institute, University of Tokyo, 1-15-1 Minamidai, Nakano-ku, Tokyo 164, Japan.

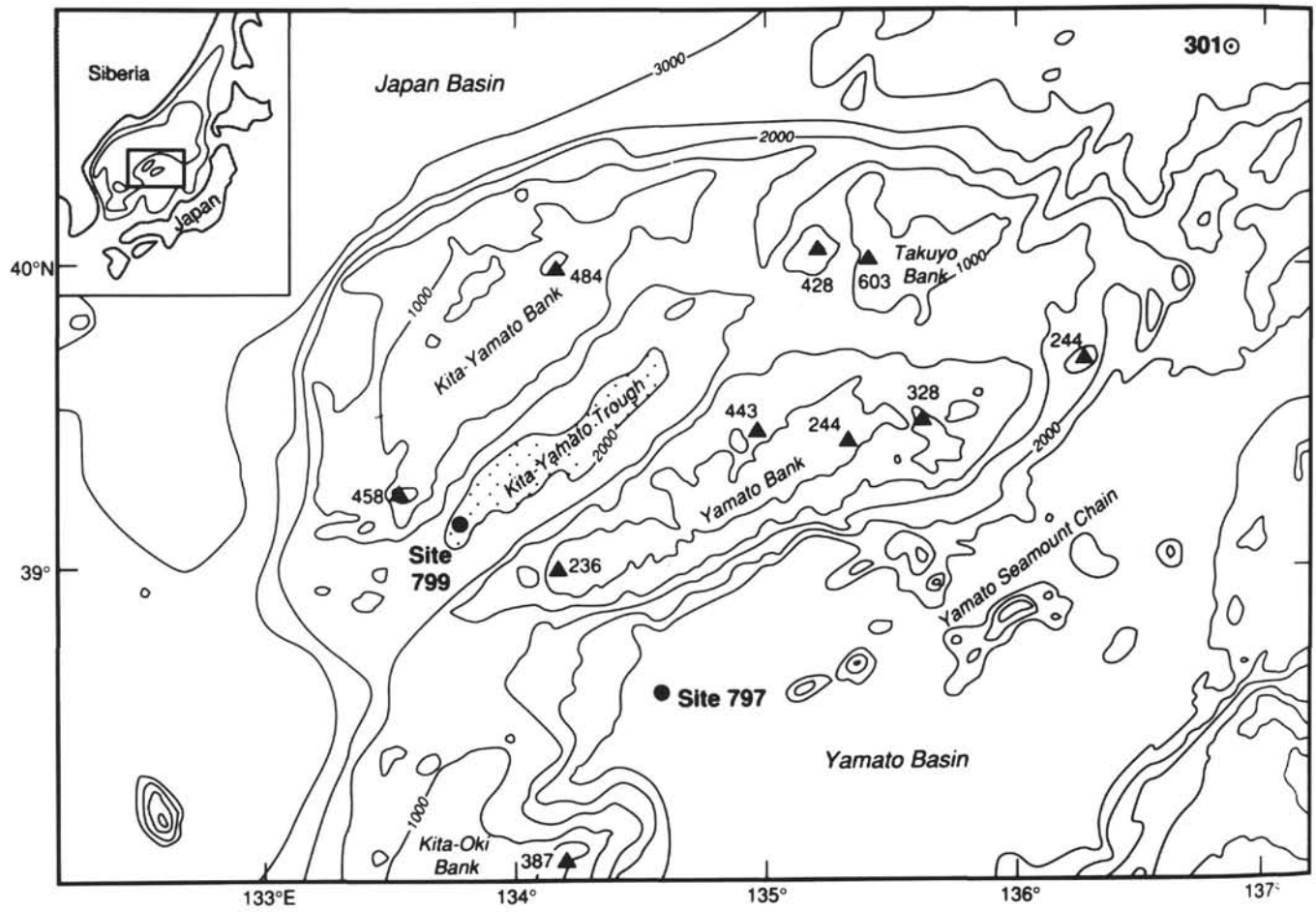

Figure 1. Bathymetric and location map of the Yamato Rise area and Site 799, south central Japan Sea. Note that the Yamato Rise consists of four discrete features: Yamato Bank, Kita-Yamato Bank, Takuyo Bank, and Kita-Yamato Trough. The shallowest areas on the rise are noted by triangles and associated water depths. Contour interval in meters.

conditions (Hamilton, 1976). These velocities represent, therefore, *in-situ* conditions and no further corrections were applied.

Calculation of Synthetic Seismograms

The synthetic seismograms were calculated using the computer program "NEWSEIS2," developed by Dr. Larry Mayer (Dalhousie University, Halifax). Detailed discussions on the methods for the calculation of synthetic seismograms are given by, e.g., Sheriff (1977), Mayer et al. (1986), and Hardage (1987). Therefore, only a brief review of the techniques used is given here. The steps involved in calculating the synthetic seismograms follow.

1. Calculation of acoustic impedance from velocity and density data vs. depth.
2. Conversion of depth below seafloor into two-way traveltime, using velocity data.
3. Calculation of the reflection coefficient from acoustic impedance.
4. Convolution of source function with reflection-coefficient log to generate synthetic seismogram.

Mayer et al. (1986) pointed out that the modeling algorithm used to generate these synthetic seismograms assumes that we are dealing with normally incident plane waves, that no energy is lost to attenuation, and that interbed multiples play no significant role.

Characteristics of the Seismic Sections in the Kita-Yamato Trough

Figures 4 to 7 show the processed seismic records obtained by the post-site survey in the Kita-Yamato Trough. Based on these records, the following seismic intervals can be distinguished: (1) the uppermost interval consists of two layers including a well stratified layer that parallels the bathymetry of the trough and a less stratified layer beneath, (2) a second relatively transparent interval which also parallels the sediment surface with the base of this interval representing the most obvious boundary within the Kita-Yamato Trough (Figs. 4-7), (3) a more reflective interval, (4) a fourth interval marked by a band of strong reflections within which individual reflectors are deformed but continuous, (5) a fifth interval similar to the third interval but more transparent toward the southeast margin of the Kita-Yamato Trough, and (6) and a band of strong reflections (acoustic basement).

In the vicinity of Site 799, seismic interval 1 reaches down to about 0.3 s two-way traveltime (twt). The upper, well stratified part of this seismic interval is situated between the seafloor and about 0.15 s twt. The seismic transparent zone of interval 2 extends down to 0.58 s. The more reflective interval 3 was found between 0.58 s and 0.93 s twt. Interval 4 reaches down to about 1.15 s, whereas interval 5 is situated between 1.15 s and acoustic basement (1.4–1.5 s twt).

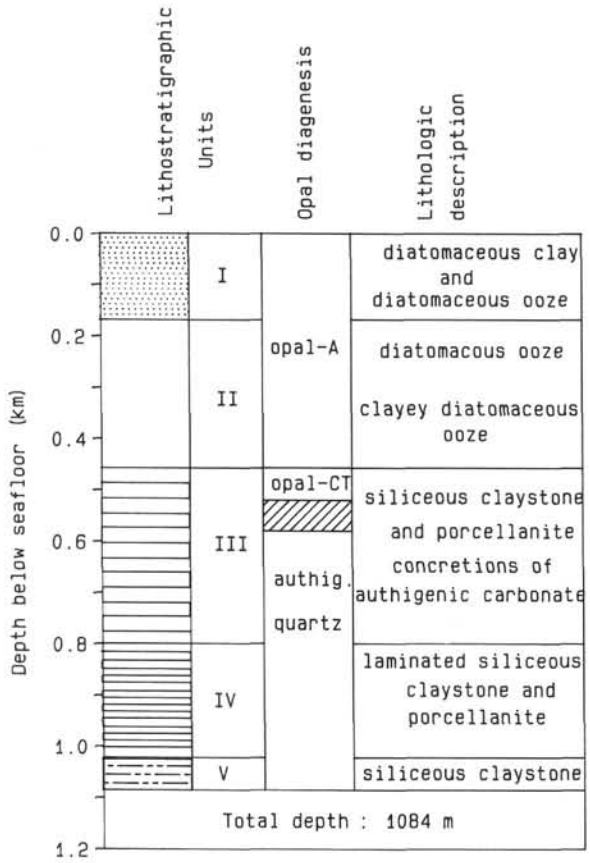

Figure 2. Summary stratigraphic column of ODP Site 799.

Geologic Model from Physical Properties

As pointed out earlier, wet-bulk density and *P*-wave velocity are the most critical physical properties for seismic modeling. The down-section variation of these properties is described in detail by the Shipboard Scientific Party (1990c). Figure 8 shows wet-bulk density and *P*-wave velocity vs. sub-bottom depth. The wet-bulk density profile was divided by the Shipboard Scientific Party (1990c) into four different units; in unit 1 (0–123 mbsf) wet-bulk density generally increases with increasing depth below seafloor. Unit 2 reaches from 123 to 320 mbsf; wet-bulk density decreases with increasing depth. The depth interval from 320 to 450 mbsf (unit 3) is characterized by an increase of wet-bulk density. At the base of this unit, wet-bulk density shows a remarkable increase from values in the range of 1.50 g/cm^3 in unit 3 to densities values of about 1.80 g/cm^3 in the upper part of unit 4. The wet-bulk densities of unit 4 (450–1084 mbsf) generally increase with increasing depth below seafloor. Many spikes are observed in the wet-bulk density profile of this unit.

P-wave velocity shows a more or less uniform increase from the seafloor to a depth of 450 mbsf (Fig. 8). At a depth of 450 mbsf a spike in velocity is observed. From this depth velocity generally increases with increasing depth below the seafloor. Many spikes in *P*-wave velocity are observed from 600 mbsf to total depth of 1084 mbsf (Fig. 8).

P-wave velocity and wet-bulk density profiles were then used to calculate the acoustic impedance (the product of velocity and density) as a function of traveltime (Fig. 9). A closer inspection of the impedance profile reveals, that the upper part (0–0.56 s twt) is more strongly influenced by wet-bulk density, whereas the lower part mirrors variations in velocity. In order to figure out the influence of density and velocity to the impedance profile, a linear regression was performed for the four physical properties units described earlier. The density/impedance regression yielded for unit 1 a R^2 value of 0.91, unit 2 is characterized by a value of 0.74. R^2 values for units 3 and 4 are 0.21 and 0.46. The velocity/impedance regression for unit 1 resulted in a R^2

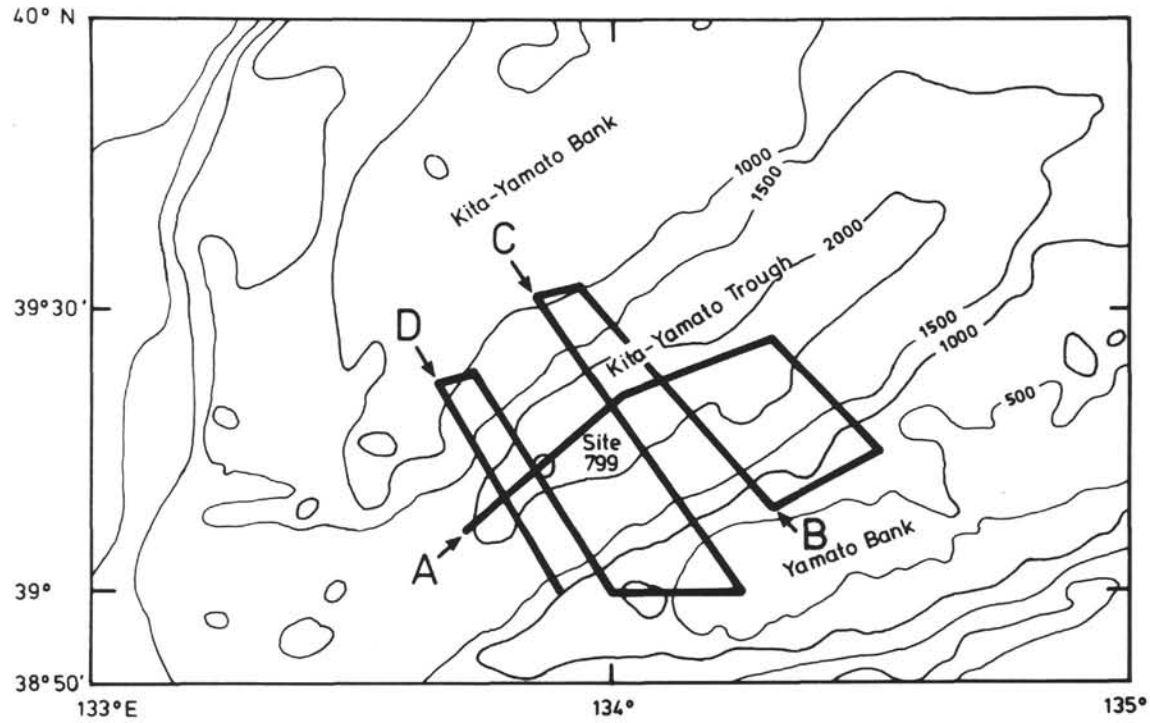

Figure 3. Location of reflection seismic profiles in the Kita-Yamato Trough (A, Fig. 4; B, Fig. 5; C, Fig. 6; D, Fig. 7).

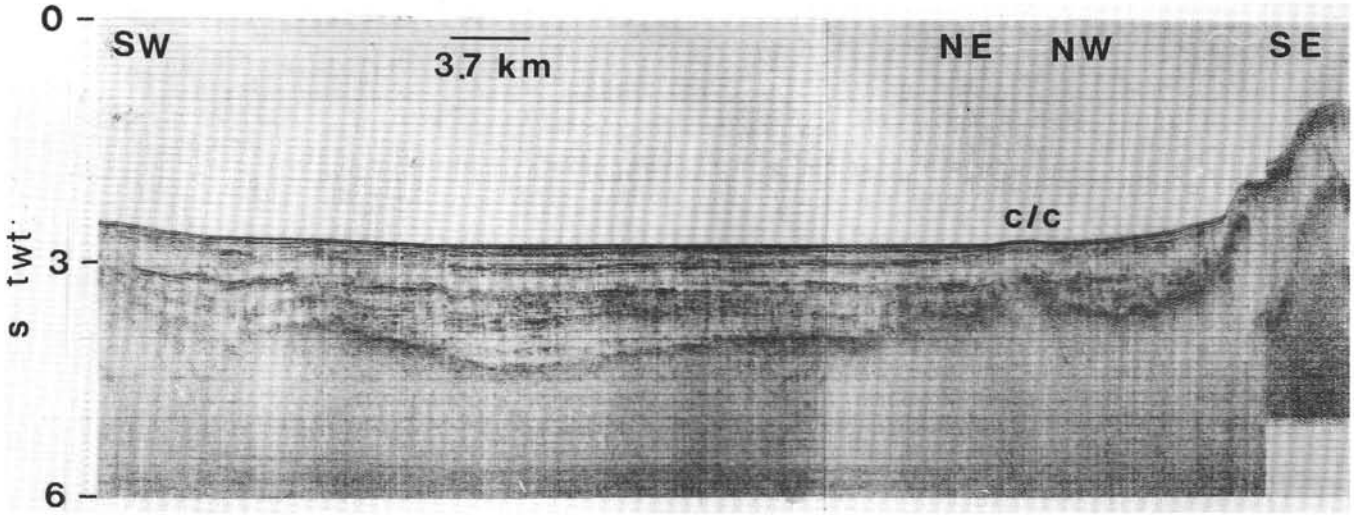

Figure 4. Seismic profile (SW/NE) from the Kita-Yamato Trough. Note course change (c/c to NW/SE). Location A in Figure 3.

value of 0.11. The regression calculated for unit 2 yielded a value of only 0.01. Units 3 and 4 show better correlation coefficients. The R^2 values are 0.47 for unit 3 and 0.92 for unit 4. From the correlation coefficients for the four physical properties units, it can be concluded that wet-bulk density variations in the upper part of Site 799 strongly affect the impedance curve. The good correlation between density and impedance for the upper part of the profile is in agreement with the findings of, e.g., Mayer (1979a,b), Mayer et al. (1986) for the central equatorial Pacific; Mienert (1986) for the eastern equatorial Atlantic; Hempel (1989) for the North Atlantic; and Holler (1989) for the southeast and east China Seas.

The key parameter to seismic profiling is the reflection coefficient. As pointed out, e.g., by Sheriff (1977) and Mayer et al. (1986), for normal incidence the reflection coefficient can be expressed in terms of impedances of the media involved. Figure 10 shows the reflection coefficient as a function of two-way traveltime. With increasing two-way traveltime below the seafloor the reflection coefficient profile can be described as follows. The upper 0.3 s twt of the reflection coefficient profile are characterized by closely spaced variations. In the section from 0.3 s twt to about 0.55 s twt only minor variations of the reflection coefficient occur. The amplitude of the reflection coefficient is very low in this section. Below 0.55 s twt a lot of high amplitude variations can be seen on the reflection coefficient vs. traveltime profile.

The convolution of the reflection coefficient vs. traveltime profile with a source function (the seismic wavelet) yields a synthetic seismo-

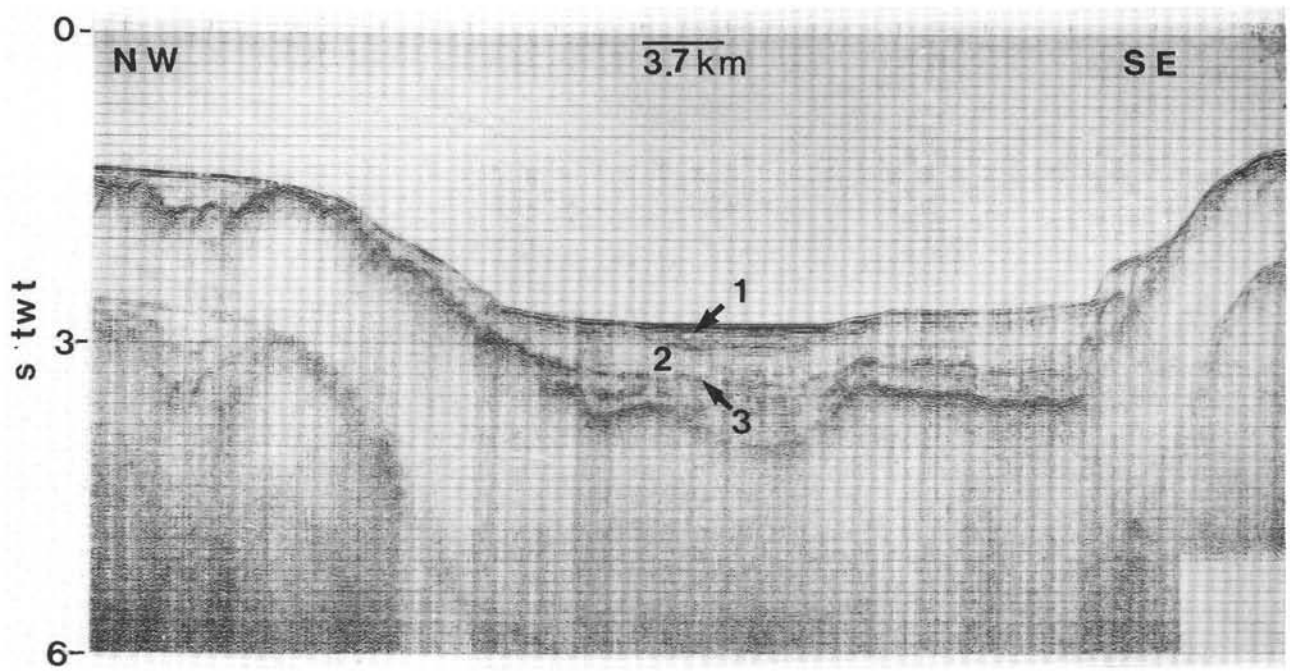

Figure 5. Seismic profile (SE/NW) across the Kita-Yamato Trough (1, seismic interval 1; 2, seismic interval 2; 3, strong reflector caused by opal-A/opal-CT transformation). Location B in Figure 3.

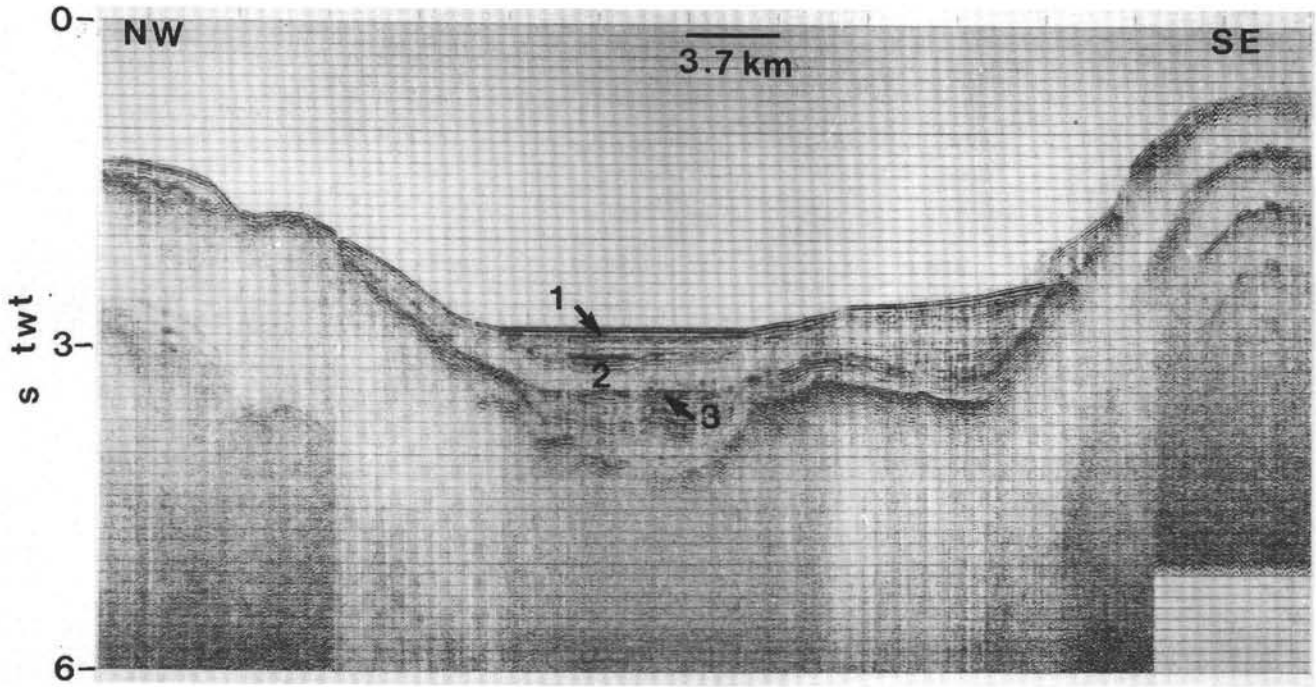

Figure 6. Seismic profile (SE/NW) across the Kita-Yamato Trough (1, seismic interval 1; 2, seismic interval 2; 3, strong reflector caused by opal-A/opal-CT transformation). Location C in Figure 3.

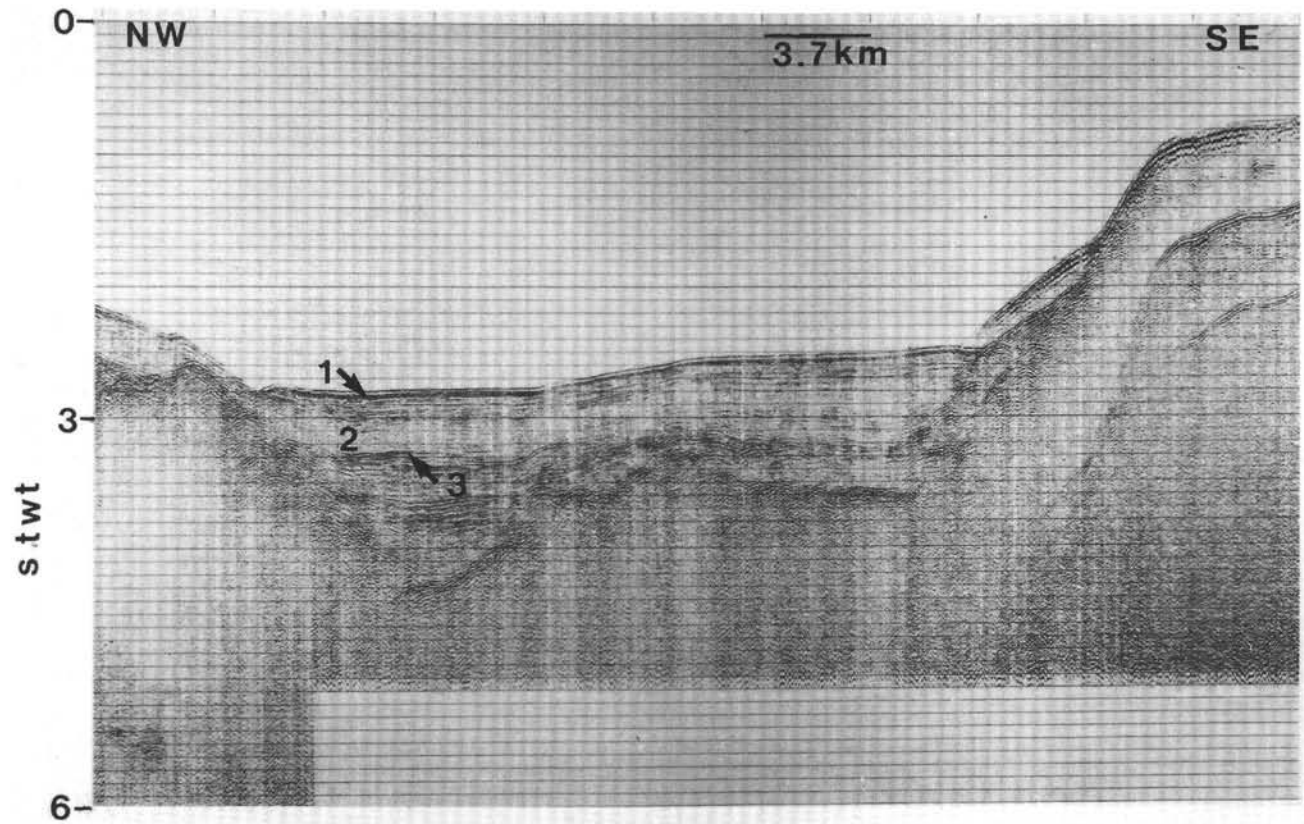

Figure 7. Seismic profile (SE/NW) across the Kita-Yamato Trough (1, seismic interval 1; 2, seismic interval 2; 3, strong reflector caused by opal-A/opal-CT transformation). Location D in Figure 3.

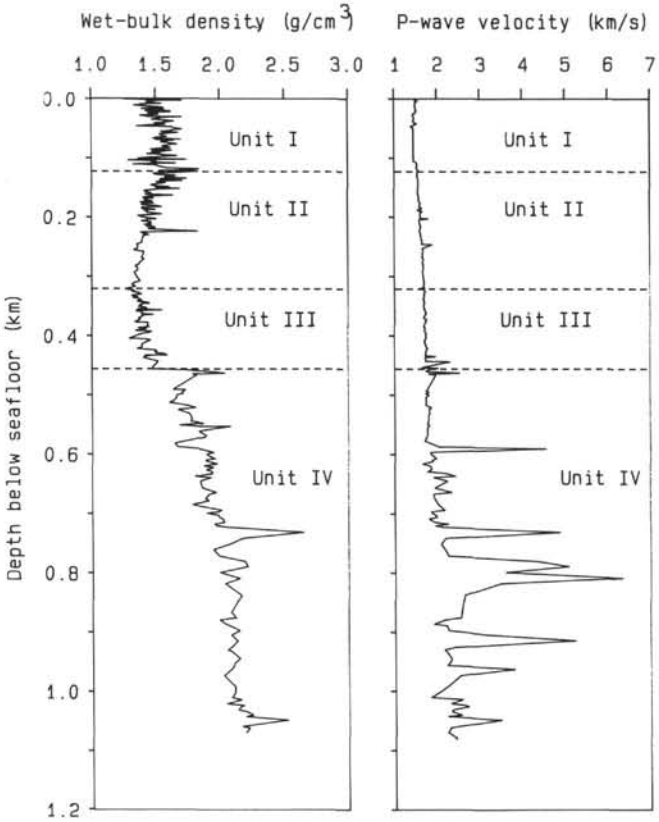

Figure 8. Wet-bulk density (left) and *P*-wave velocity (right) vs. sub-bottom depth, Site 799. Units I to IV are physical property units.

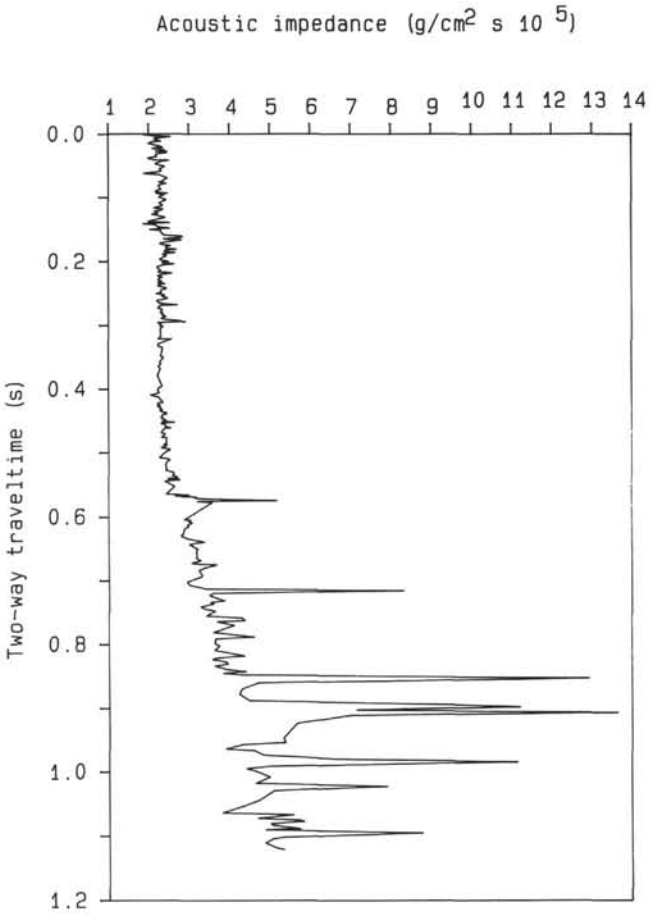

Figure 9. Acoustic impedance vs. two-way traveltime, Site 799.

gram. Figure 11 shows a comparison of the seismic field record and the calculated synthetic seismogram. The comparison of the field record and the synthetic seismogram clearly shows that the major reflections in both records agree well. This agreement indicates that our geologic model—expressed as impedance profile and synthetic seismogram—can be used to (1) explain the origin of reflectors in the field record, and (2) tie the seismic information on the Kita-Yamato Trough to the lithology and stratigraphy as obtained by the drilling record of Site 799.

ORIGIN OF REFLECTORS

Reflectors in Seismic Intervals 1 and 2

As noted earlier, seismic intervals 1 and 2 reach down to about 0.58 s twt. The sub-bottom depth to traveltime conversion of Site 799 core data reveals that 0.58 s twt (the base of seismic interval 2) is equivalent to a depth of about 458 mbsf, the base of lithostratigraphic unit 2 and physical property unit 3. The base of seismic interval 1 (0.30 s twt) does not coincide with the boundary of a lithostratigraphic or physical property unit.

The comparison of the well stratified section of seismic interval 1 (0–0.15 s twt) and the wet-bulk density profile reveals that density shows small scale variations. The depth to traveltime conversion shows that the stratified interval reaches down to about 117 mbsf. In this depth interval more or less terrigenous sediments showing distinctive light/dark rhythms were described (Shipboard Scientific Party, 1990c), causing the observed small scale variations of wet-bulk density. The depth of 110 mbsf is 13 m above the base of physical property unit 1 (123 mbsf). An acoustic transparent part exists within the upper stratified interval (about 0.05–0.10 s twt). The depth of this transparent zone (about 38–75 mbsf) coincides with an interval of Site 799 where typically debris flow deposits were recovered. The lower, less stratified section of seismic interval 1 (0.15–0.3 s twt; 110–230 mbsf) crosses the base of lithology unit 1 (170 mbsf). In the upper part of lithology unit 2, sediments contain less terrigenous detritus but more biosilica, like diatoms. The wet-bulk density in this depth interval still shows fluctuations but is generally decreasing with increasing depth below seafloor.

Comparing seismic interval 1 of the field record with the impedance curve, it becomes clear that the observed parallel reflectors do not directly represent impedance changes in the sediment section. The reflectors are interference patterns resulting from the interaction between the closely spaced impedance contrasts and the seismic wavelet. Such interference patterns were also described by Mayer (1979b) for deep-sea carbonates in the equatorial Pacific.

Seismic interval 2 reaches from 0.3 s twt to 0.58 s twt (230–460 mbsf). This interval shows up as a transparent zone on the field record. The depth range of seismic interval 2 coincides with the lower part of lithostratigraphic unit 2. The sediments recovered from the depth interval of 230–458 mbsf are characterized by an increasing amount of siliceous microfossils in the depth range between 230 and 320 mbsf. From this depth the amount of siliceous microfossils is decreasing toward the depth of 458 mbsf. Wet-bulk densities within this depth interval show in the upper part (230–320 mbsf) a decrease with increasing depth below seafloor. From a depth of 320 mbsf, wet-bulk densities increase with increasing depth. Physical property unit 2 and unit 3 are based on this behavior of wet-bulk density. The apparent reason for the decrease of wet-bulk density with increasing depth is the high amount of biogenic opaline within this depth interval (see Nobes et al., this volume). The reflection coefficient profile of this section shows only minor contrasts. This leads to the acoustic trans-

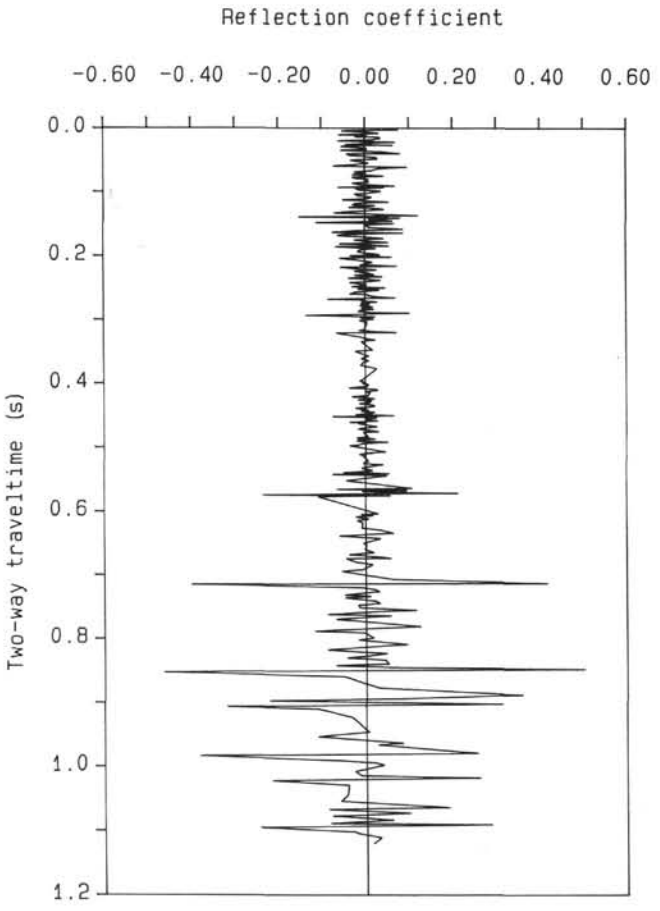

Figure 10. Reflection coefficient vs. two-way traveltime, Site 799.

parent zone, seen on the field record. A similar acoustic transparent zone in seismic records from the north Atlantic Ocean has been shown by Hempel (1989) to be typically for sediments rich in biogenic opaline. The strong reflector at the base of seismic interval 2 correlates with the base of lithologic unit 2 and physical property unit 3 (Shipboard Scientific Party, 1990c). Sediments recovered from the depth interval of about 458 mbsf are characterized by the diagenetic transformation from opal-A (biogenic opaline, like diatom frustules) to opal-CT. This diagenetic transformation causes a dramatically increase of wet-bulk density, leading to the strong impedance contrast, responsible for the generation of the reflector seen in the field record and in the synthetic seismogram. As seen in the seismic records, this reflector can be traced in the whole area of the Kita-Yamato trough. The transformation from opal-A to opal-CT is generally much more influenced by the heat flow than by pressure (e.g., Riech and von Rad, 1979). So the opal-A/opal-CT reflector can be used as an indicator of the thermal structure of the area (see Kuramoto et al., this volume).

Reflectors in the Lower Section

As pointed out above, the impedance profile of the lower part of section of Site 799 is strongly influenced by sonic velocity. Seismic interval 3 reaches from 0.58 s twt to about 0.90 s twt (458–799 mbsf). The seismic interval coincides with lithostratigraphic unit 3 (458–800 mbsf). The sediments of this unit consist of siliceous claystone and porcellanite, intercalated with beds, laminae, and concretions of authigenic carbonate (Shipboard Scientific Party, 1990c). This interval also includes the diagenetic transition from opal-CT to quartz at a depth of 585 mbsf. An inspection of the impedance log of this unit reveals many spikes in impedance values, caused mainly by high velocities. It is interesting to note, that the opal-CT/quartz transition at a depth of about 585 mbsf is not characterized by an increasing wet-bulk density, but that a high sonic velocity was recorded. As pointed out by the Shipboard Scientific Party (1990c), the spikes in velocity and density in the depth range between 700 and 800 mbsf are due to frequent dolomite stringers in this depth interval. These dolomite stringers cause a high impedance contrast and are responsible for the generation of reflectors within seismic unit 3.

Seismic unit 4 ranges from about 0.90 s twt and 1.15 s twt (800 mbsf to total depth of 1084 mbsf). This section includes the lithostratigraphic units 4 (800–1020 mbsf) and 5 (1020–1084 mbsf). The sediments recovered from this depth interval consist of finely laminated to thinly bedded siliceous claystone and porcellanite (unit 4) and siliceous claystone and claystone with silt (unit 5). Of special interest is a gray, altered sequence of rhyolitic tuff from 981 to 1002 mbsf, because this sequence is similar to rhyolitic rocks associated with the Miocene Kuroko massive sulfide deposits in northern Japan (Sato, 1974).

The wet-bulk density is not significantly higher in the zone, where the rhyolitic tuff is deposited, but sonic velocity decreases within this layer. Generally seismic interval 4 is characterized by closely spaced reflections. Looking at the lithology of this depth interval, it is clear, that the reflectors within this depth interval are interference patterns, like the reflectors seen in seismic interval 1.

Regional Geological Implications

A comparison of the successful correlation of seismic and lithologic units from the Kita-Yamato Trough with the more regional results of extensive single channel seismic reflection data (Tamaki, 1988), drilling results from DSDP Leg 31 (Karig, Ingle, et al., 1975), and ODP Leg 127 (Tamaki, Pisciotto, Allan, et al., 1990) will provide information on the sedimentation and sediment diagenesis in the Japan Sea.

The Shipboard Scientific Party (1990b) stated that a typical basinal sequence includes (1) an upper well-stratified and highly reflective unit composed of upper Pliocene to Holocene siliciclastic sands, silts, and/or clays overlying (2) a seismically transparent to moderately reflective unit of lower Pliocene to Miocene hemipelagic diatomaceous clays and other mud rocks. Drilling at DSDP Site 301 early confirmed that acoustically transparent subunits in the upper portions of these sediments represent Pliocene to upper Miocene diatomaceous oozes and muds (Karig, Ingle, et al., 1975).

Tamaki, Pisciotto, Allan, et al. (1990) identified at each site of ODP Leg 127 four or five seismic intervals above the opaque basement. These seismic intervals are broadly similar in seismic character, and at least three types of intervals occur: (1) those characterized by reflections which originate from stratal facies; (2) those originated from pronounced diagenesis of the diatomaceous lithofacies; and (3) acoustic basement covered by stratified opaque interval. Tamaki, Pisciotto, Allan, et al. (1990) also pointed out that diatomaceous ooze represents a transparent interval and alternated cherts and siliceous claystones below the opal-A/opal-CT diagenetic front represent well-stratified layers, both of which are commonly observed in the basin margin areas of the Japan Sea.

The local reflection pattern from the Kita-Yamato Trough, as documented in Figures 3–7, is in good agreement with the regional reflection pattern of the Japan Sea.

Reflectors caused by the diagenetic opal-A/opal-CT boundary can be traced over large parts of the Japan Sea and provide information about the thermal history of this regions.

Upper Miocene to upper Pliocene biosiliceous sediments above the opal-A/opal-CT diagenetic boundary reflect an increase in diatom

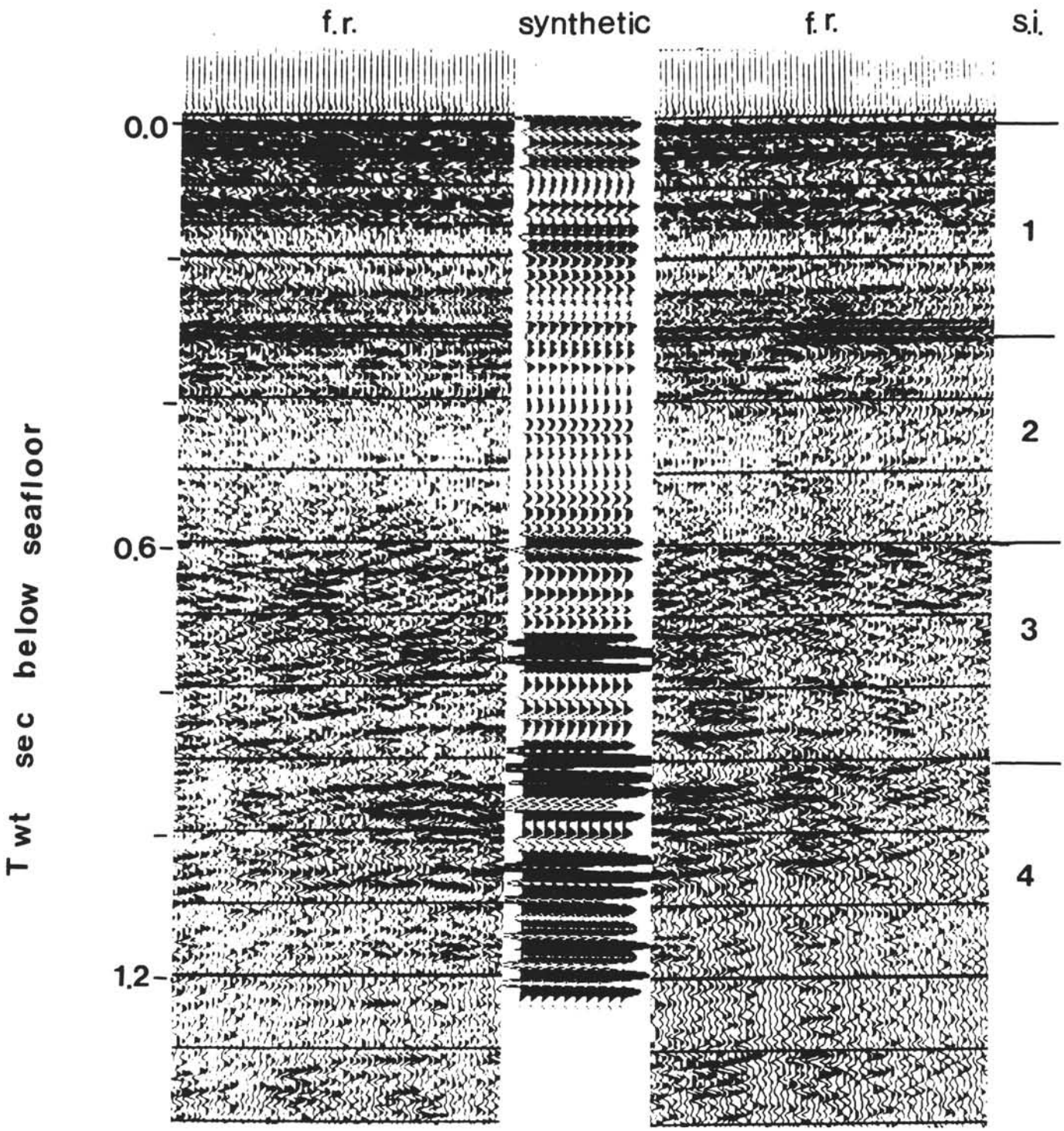

Figure 11. Comparison between seismic field record (f.r.), synthetic seismogram (synthetic), and seismic intervals (s.i.) in the vicinity of Site 799.

productivity and imply a generally good basin circulation and oxic bottom water condition in this period. These sediments can be correlated to a transparent seismic interval.

The well-stratified and highly reflective upper unit in the Japan Sea mirrors a change in sedimentation. The sediments are generally more influenced by terrigenous material. Dark/light rhythms in the upper part of section (Föllmi et al., this volume) are assumed to express rapid changes in the paleoceanographic regime of the Japan Sea.

CONCLUSIONS

The analysis of high resolution seismic reflection data from the Kita-Yamato Trough enabled us to differentiate five seismic intervals above acoustic basement. A geologic model, constructed from physical property data was used to calculate a synthetic seismogram in order to correlate the borehole information with the seismic field record. Using borehole data it is possible to identify the origin of

seismic intervals 1 to 4. This correlation led to the following results (see also Fig. 12).

The well stratified reflectors of seismic interval 1 are caused by the interference of the seismic wavelet with the highly variable reflection coefficient profile. A seismic transparent zone within this interval is caused by debris flow deposits.

Seismic interval 2 is characterized by a transparent layer. This seismic transparency is caused by a low impedance contrast due to a high portion of siliceous microfossils within the sediments.

An increase in wet-bulk density and *P*-wave velocity due to the diagenetic transformation from opal-A to opal-CT is responsible for the generation of a strong reflector. This reflector can be traced across the whole Kita-Yamato Trough.

Reflectors in seismic interval 3 monitor stringers of authigenic dolomite, characterized by higher wet-bulk densities and *P*-wave velocities.

The parallel reflectors of seismic interval 4 are also interpreted as interference pattern. The sediments recovered at Site 799 consist of laminated to thinly bedded siliceous claystone and porcellanite.

ACKNOWLEDGMENTS

We would like to thank the crew of *JOIDES Resolution* for their assistance and cooperation during Leg 128. Dr. Larry Mayer (Dalhousie University) kindly provided the program for calculating the synthetic seismograms. PRH acknowledges the financial support provided by the German Science Foundation (Deutsche Forschungsgemeinschaft).

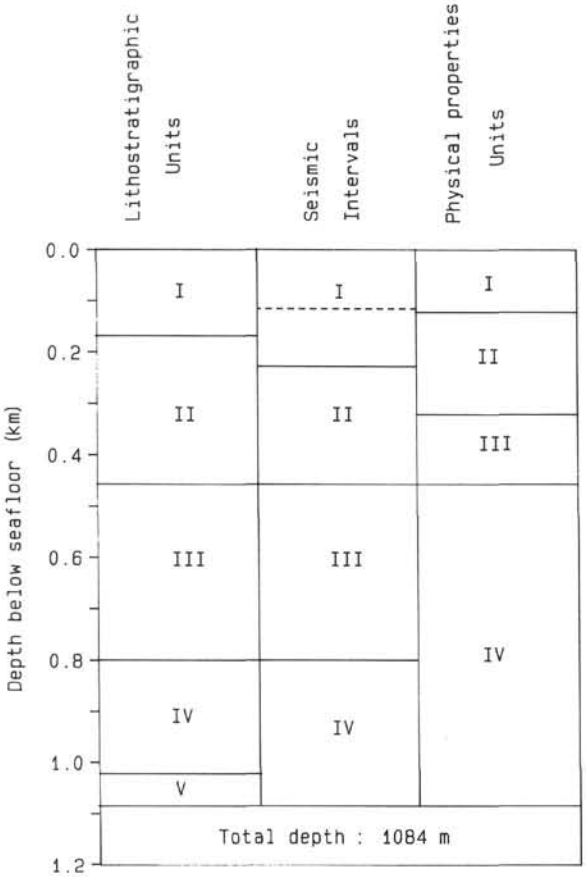

Figure 12. Correlation between lithostratigraphic units, seismic intervals, and physical property units, Site 799.

REFERENCES

Borehole Research Group, 1987. *Wireline Logging Manual* (2nd ed.): New York (Lamont-Doherty Geol. Observatory, Columbia Univ.).

Boyce, R. E., 1976. Definitions and laboratory techniques of compressional sound velocity parameters and wet-water content, wet-bulk density, and porosity parameters by gravimetric and gamma ray attenuation techniques. *In* Schlanger, S. O., Jackson, E. D., et al., *Init. Repts. DSDP,* 33: Washington (U.S. Govt. Printing Office), 931–958.

Hamilton, E. L., 1976. Variations of density and porosity with depth in deep-sea sediments. *J. Sediment. Petrol.,* 46:280–300.

Hardage, B. A., 1987. Seismic stratigraphy. *In* Helbig, K., Treitel, S. (Eds.), *Handbook of Geophysical Exploration* (Vol. 1): *Seismic Exploration:* Amsterdam (Geophysical Press), 9.

Hempel, P., 1989. Der Einfluß von biogenem Opal auf die Bildung seismischer Reflektoren und die Verbreitung opalreicher Sedimente auf dem Voering Plateau. *Ber. Sonderforschung. 313, Univ. Kiel,* 14.

Holler, P., 1989. Akustische Eigenschaften von Beckensedimenten aus dem Süd- und Ostchinesischen Meer. *In* Degens, E. T. (Ed.) *Wiss. Ber. Forschungsschiff "Sonne" Reise 50:* Hamburg.

Karig, D. E., Ingle, J. C., Jr., et al., 1975. *Init. Repts. DSDP,* 31: Washington (U.S. Govt. Printing Office).

Mayer, L. A., 1979a. Deep sea carbonates: acoustic, physical, and stratigraphic properties. *J. Sediment. Petrol.,* 49:819–836.

———, 1979b. The origin of fine scale acoustic stratigraphy in deep sea carbonates. *J. Geophys. Res.,* 84:6177–6184.

Mayer, L. A., Shipley, T. H., Theyer, F., Wilkens, R. H., Winterer, E. L., 1986. Seismic modeling and paleoceanography at Deep Sea Drilling Project Site 574. *In* Mayer, L. A., Theyer, F., Thomas, E., et al., *Init. Repts. DSDP,* 85: Washington (U.S. Govt. Printing Office), 947–970.

Mienert, J., 1986. Akustostratigraphie im äquatorialen Ostatlantik: Zur Entwicklung der Tiefenwasserzirkulation der letzten 3,5 Millionen Jahre. *"Meteor" Forschungsergeb. Reihe C,* 40:19–86.

Riech, V., von Rad, U., 1979. Silica diagenesis in the Atlantic Ocean: diagenetic potential and transformations. *In* Talwani, M., Hay, W., Ryan, W.B.F. (Eds.), *Deep Drilling Results in the Atlantic Ocean: Continental Margins and Paleoenvironment.* Am. Geophys. Union, Maurice Ewing Ser., 3:315–340.

Sato, T., 1974. Distribution and geological setting of the Kuroko deposits. *In* Ishihara, S., et al. (Eds.), *Geology of Kuroko deposits.* Min. Geol., Spec. Iss., 6:1–9.

Sheriff, R. E., 1977. Limitations on resolution of seismic reflections and geologic details derivable from them. *In* Payton, C. E. (Ed.), *Seismic Stratigraphy—Applications to Hydrocarbon Exploration.* AAPG Mem., 26:3–14.

Shipboard Scientific Party, 1990a. Explanatory Notes. *In* Ingle, J. C., Jr., Suyehiro, K., von Breymann, M. T., et al., *Proc. ODP, Init. Repts.,* 128: College Station, TX (Ocean Drilling Program), 39–64.

———, 1990b. Introduction, background, and principal results of Leg 128 of the Ocean Drilling Program, Japan Sea. *In* Ingle, J. C., Jr., Suyehiro, K., von Breymann, M. T., et al., *Proc. ODP, Init. Repts.,* 128: College Station, TX (Ocean Drilling Program), 5–38.

———, 1990c. Site 799. *In* Ingle, J. C., Jr., Suyehiro, K., von Breymann, M. T., et al., *Proc. ODP, Init. Repts.,* 128: College Station, TX (Ocean Drilling Program), 237–402.

Tamaki, K., 1988. Geological structure of the Japan Sea and its tectonic implications. *Chishitsu Chosasho Geppo,* 39:269–365.

Tamaki, K., Pisciotto, K., Allan, J., et al., 1990. *Proc. ODP, Init. Repts.,* 127: College Station, TX (Ocean Drilling Program).

Date of initial receipt: 18 May 1991
Date of acceptance: 28 February 1991
Ms 127/128B-234